https://doi.org/10.15407/ujpe68.1.38

I.M. KUPCHAK, D.V. KORBUTYAK

V. Lashkarev Institute of Semiconductor Physics, NAS of Ukraine
(45, Prospect Nauky, Kyiv 03680, Ukraine; e-mail: kupchak@isp.kiev.ua)

SPECTRAL CHARACTERISTICS OF PASSIVATED CdTe QUANTUM DOTS WITH COORDINATE-DEPENDENT PARAMETERS

Theoretical studies of the energy spectrum of quantum dots are often carried out using the effective mass approximation with the parameters of the calculation set by the corresponding values of the bulk material of both the dot itself and its surroundings. In this study, the effective mass is a coordinate-dependent function, and its dependence on the coordinate is determined by the atomic structure of the quantum dot, which, in turn, is calculated by the density functional method. Both an unpassivated quantum dot and one passivated with thiol-glycolic acid are considered.

K e y w o r d s: quantum dots, coordinate-dependent effective mass, cadmium telluride.

1. Introduction

Quantum dots (QDs) of A_2B_6 semiconductors are an important material for the use in light-emitting devices, in the magnetic resonance imaging as a "contrasting" material for a medical purpose, and for the targeted drugs delivery to diseased cells [1]. Another important field of applications of quantum dots is photovoltaics, where they are used as a material for solar cells – QDSCs [2], as well as for solar light concentrators (LSCs) [3]. Such advantages are provided by the spatial confinement effect, which is most significant in zero-dimensional semiconductor QDs and provides a unique possibility to change the band gap and, accordingly, to obtain a wide range of luminescence spectra (from blue to red) with a high quantum yield. Due to these circumstances, in general, there is a tendency to increase the efficiency of the application of such QDs in various photovoltaic systems [4].

Usually, QDs A_2B_6 are manufactured by methods of colloidal chemistry, the so-called "wet technologies". The nanocrystals obtained by such methods have dangling bonds, because the crystal order is broken on the surface, and the external atoms do not have the correct surround. As a result, the colloidal solution quickly coagulates, precipitates, and no longer exhibits the typical characteristic of nanocrystals. To avoid this, nanocrystals are passivated with certain stabilizers that saturate the QD surface, and thus prevents the formation of chemical bonds between nanocrystals. Thereby, in addition to the problem of studying the characteristics of the nanocrystals themselves, there is another problem of studying the influence of a passivator on the properties of the nanocrystal. At the same time, there is an uncertainty arising in comparisons of the results of theoretical calculations with experimental data: it is unclear how to define the size of a nanocrystal and how to match a theoretical model (cluster) to a real quantum dot. Therefore, many works are devoted to the study of both the QDs themselves and the fea-

C i t a t i o n: Kupchak I.M., Korbutyak D.V. Spectral characteristics of passivated CdTe quantum dots with coordinate-dependent parameters. *Ukr. J. Phys.* **68**, No. 1, 38 (2023). https://doi.org/10.15407/ujpe68.1.38.

Ц и т у в а н н я: Купчак І.М., Корбутяк Д.В. Спектральні характеристики пасивованих квантових точок CdTe з координатно-залежними параметрами. *Укр. фіз. журн.* **68**, № 1, 38 (2023).

tures of the use of passivators (see the review [5] and the list of references therein).

In recent years, an interest in ultrasmall (less than 2 nm) quantum dots has increased [6–12]. This subset of QDs includes magic-size clusters, containing a certain, well-defined number of atoms. Ultrasmall QDs are characterized by unique properties – sharp absorption of light and almost completely surface luminescence. They are promising for a variety of applications ranging from dye-sensitized solar cells, white light LEDs, and biological sensing due to their controllable electronic structure and band gap, as well as their large specific surface area. Thus, ZnSe QD structures have great potential for providing new optoelectrical properties due to the energy transfer from small QDs to large ones [7]. The high quantum yield of ultrasmall CdS QDs makes them attractive for the fabrication of highly sensitive biosensors [8]. The detailed study and prospects of practical applications of ultrasmall QDs require a continuous improvement of the technology of their synthesis [9–11].

From the point of view of theoretical research, there are two approaches that are most often applied to quantum dots: these are atomistic methods, such as the density functional theory, and a phenomenological model – the $k \cdot p$ or effective mass method. The former allow one to study the energy spectra and structural characteristics. However, they are limited only to small systems of up to several hundred atoms. Since the total system may include also atoms of a passivator, the calculations of even relatively small clusters with the effects of their real completely disregarded surroundings become too cumbersome. Nevertheless, such models are adequate and are able to describe real quantum dots of ultrasmall sizes [8, 13]. The latter introduces the concept of a quasiparticle and allows one to describe not only the quantum-dimensional effect, but also the effect of dielectric enhancement [14,15], interaction between different nanocrystals [16] *etc.*

The effective mass method exploits the solid-state approach for describing the nanocrystals and reduces to solving the problem of a particle in the potential well formed by the energy bands offset of the nanocrystal materials and the environment. Obviously, this approach is more suitable for describing the relatively large-sized QDs with well defined crystal structure. Effective masses and dielectric constants are step functions of coordinates and take fixed values in each material of the system. At the same time, it is believed that these materials retain "bulk" values for their characteristic parameters such as the effective electron and hole masses. However, there are no guarantees regarding this statement, since the crystal structure of nanocrystals is not always known and still is the subject of many experimental and theoretical studies. In addition, the bulk parameters are not always known in advance, so they have to be determined theoretically by other available methods based on the structural characteristics of the material [17], which, in turn, could be determined by atomistic approaches.

In particular, the structural characteristics of nonstoichiometric CdTe QDs were investigated in work [18], where the atomic structure of small clusters of $\sim$25 atoms was simulated. A considerable attention was paid to establish the influence of the interaction of individual atomic orbitals on it: due to the repulsion between p-orbitals of tellurium, the cadmium core firstly and then the tellurium surround are formed. A wider range of sizes (up to 120 atoms), both stoichiometric and nonstoichiometric, was studied in [19], where it was shown that nonstoichiometric clusters have a lower HOMO-LUMO transition energy than stoichiometric ones. In all cases, the atomic structure differed from that of the bulk material. For some sizes, calculations of several isomers were performed, which showed that the binding energy per atom for all isomers is practically the same, but the energies of the HOMO-LUMO transition are different. Obviously, this is due to a small number of atoms; so, the geometric position of each atom significantly affects the formation of the wave function (molecular orbital) and, therefore, the energy of the corresponding energy level, while the interatomic interaction (bond energy) is relatively short-range, is limited to the atoms of the immediate local environment, and, therefore, is less sensitive to the geometric structure as a whole (of course, provided that the atoms are in equilibrium positions).

Therefore, the purpose of this work is to investigate the influence of the atomic structure on the spectral characteristics of quasiparticles (electrons and holes) in quantum dots. To do this, we will a) consider the quantum dot model and study its atomic structure in details taking a cadmium telluride atomic cluster as an example, b) establish the dependence of the effective mass on the coordinate, and c) investigate the

influence of the coordinate-dependent effective mass on the energy spectrum. For the sake of simplicity, we will limit ourselves to the study of the influence of only the effective mass, although other important parameters – such as potential barriers and dielectric constants may also appear to be dependent on the local structure of the material and have a non-trivial dependence on the coordinates.

2. Computational Details

Calculations of the atomic and electronic structures of clusters were carried out by the density functional method using the hybrid exchange-correlation functional B3LYP [20] and the basis of localized orbitals LANL2DZ [21] as realized in the GAMESS-US software package [22]. The geometry optimization was carried out over all internal variables without symmetry constraints, checking the vibrational spectrum: the system was optimized, when there were no imaginary frequencies. Characteristics of bulk cadmium telluride were calculated in the local density approximation (LDA) using the QUANTUM-ESPRESSO software package [23]. Ultrasoft pseudopotentials corresponding to the configuration of valence electrons $4d^{9.5}5s^25p^{0.5}$ for cadmium and $5s^25p^4$ for tellurium were used. The Brillouin zone integration was performed using a $12 \times 12 \times 12$ grid of k-points generated by the Monkhorst–Pack [24] scheme. The expansion of the wave function was limited to the terms corresponding to the kinetic energy of 60 Ry and 1200 Ry in the region of the pseudopotential.

3. Cd_9Te_9 and $Cd_{33}Te_{33}$ Clusters Passivated by Thiol-Glycolic Acid Molecules and -SCH_3 Fragments

The initial Cd_9Te_9 cluster is chosen in the form of three hexagonal rings, as shown in Fig. 1, *a*. Such a system has C_{h3} symmetry, and all cadmium atoms belong to the surface and contain broken bonds. These broken bonds were passivated by molecules of thiol-glycolic acid (TGA) SCH_2CO_2H, the atomic structure of which is shown in Fig. 1, *b*, as well as by fragments of SCH_3 in such a way that the S–Cd bonds are formed instead of the S–H bonds. The geometric optimization of the clusters was carried out without symmetry constraints, and the final atomic structure appeared to be significantly deformed in both cases: as can be seen from Fig. 1, *c*, a significant rearrangement of chemical bonds took place during the optimization process. The length of the Cd–Te chemical bonds is in the interval 2.87– 3.15 Å, while the Cd–S bonds are somewhat shorter: 2.65–2.76 Å. The electronic charge is localized mostly on metal atoms, carbon, and lesser on sulfur atoms. The Mulliken population analysis indicates that the HOMO level is formed mainly by states of surface tellurium atoms and partially by sulfur atoms. The LUMO level is formed mainly by states of sulfur and, to a lesser degree, tellurium. Other passivator atoms (hydrogen, oxygen, carbon) practically do not contribute to the formation of HOMO-LUMO levels. This is clearly seen from the calculated partial density of electronic states, depicted in Fig. 1, *e*: HOMO-LUMO levels are formed by states of tellurium and sulfur atoms, although the LUMO level also includes states of carbon atoms. Oxygen and hydrogen form states far from these levels; so, in the further calculations, it is advisable to use fragments of the TGA SCH_3 molecule as a passivator model. This will reduce the total number of atoms to precisely those atoms whose states are "important" for the optical transition.

It is worth to note that the energy distance between the HOMO-LUMO levels, which is analogous to the band gap in bulk semiconductors, is 2.52 eV. In the non-passivated optimized cluster (not shown), a clear band gap of 2.76 eV is also observed. This result is typical of stoichiometric systems [19], when, in the process of geometric optimization, surface bonds are rearranged to minimize the number of broken bonds (i.e., "self-healing"). That is why the passivation does not necessarily lead to an improvement in the energy structure of a cluster, but is important for preventing the coagulation and for stabilizing the entire colloidal solution.

The $Cd_{33}Te_{33}$ cluster is obtained by "cutting out" an approximately spherical region of a bulk cadmium telluride with the wurtzite crystal structure, keeping only those atoms with at least two chemical bonds. The center of the cluster is chosen at the middle of the Cd–Te chemical bond to ensure the stoichiometry of the system. Surface cadmium atoms with broken bonds were passivated by fragments of the SCH_3 in the same way as during the passivation of the Cd_9Te_9 cluster by original TGA molecules. The atomic structures of the optimized $Cd_{33}Te_{33}$ and $Cd_{33}Te_{33} : (SCH_3)_{21}$ clusters are shown in Fig. 1, *d* and *f*, respectively.

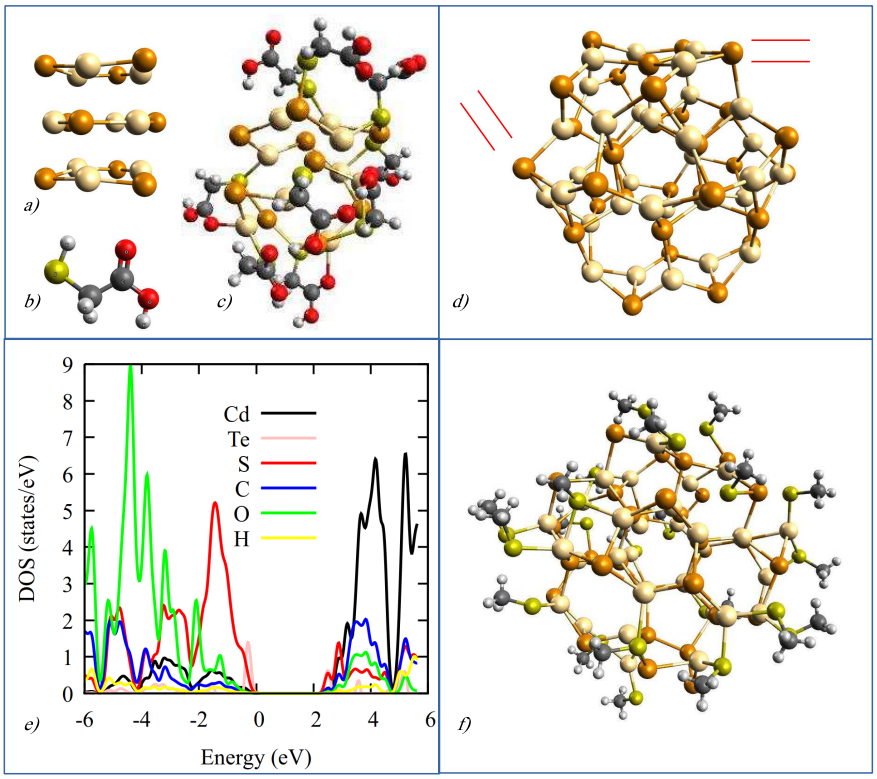

Fig. 1. (Color online) Schematic representation of the optimized atomic structure of the Cd_9Te_9 cluster (*a*), the thiol-glycolic acid molecule (*b*), the $Cd_9Te_9 : (SCH_2CO_2H)_9$ cluster (*c*), cluster $Cd_{33}Te_{33}$ (*d*), cluster $Cd_{33}Te_{33} : (SCH_3)_{21}$ (*f*) and the partial density of electronic states of individual sorts of atoms (*e*). Sulfur is marked in yellow, cadmium in light yellow, tellurium in brown, oxygen in red, carbon in gray, and hydrogen in light gray

As is seen from the figure, both optimized clusters have a crystal structure close to the structure of zinc blende. In an unpassivated cluster, certain faces are formed at the surface, marked with red dashes, on which the atoms align and form a quasi-two-dimensional layer: the chemical bonds in the direction toward the center of the cluster are elongated to values of ∼3.6 Å and more, exceeding significantly the average bond length ∼2.8 Å in the inner part. Such faces are not observed in the passivated cluster. For an unpassivated $Cd_{33}Te_{33}$ cluster, the radius (the largest distance from the geometric center of the cluster to its outer atom) is 8.128 Å, and, for a passivated one (without accounting for the molecules of a passivator) – 8.643 Å. Such a difference in size is due to the shortening of the length of chemical bonds at the surface of the unpassivated cluster, while, for the passivated cluster at the surface, additional Cd–S bonds prevent a strong reconstruction of the geometric structure.

Figure 2 shows the dependence of the length of Cd–Te chemical bonds on the relative position of the center of this bond in the cluster. As we can see, the bond length can both increase and decrease. Red lines show the average of positive deviations, and blue lines – negative ones. For an unpassivated cluster (Fig. 2, *a*), the length of chemical bonds varies unevenly: it firstly increases with the distance from the center and rapidly decreases on the surface. This is clearly followed by positive deviations: the red line firstly goes up, and, in the near-surface region, it returns back to the region of shorter lengths. At the same time, the blue line changes more slightly, since the geometric centers of most bonds are on the surface of the cluster. As a result, the overall averaging of bond lengths (black line) practically reproduces the behavior of the red line. This corresponds to the picture of the formation of faces: one part of the chemical bonds breaks down, and other part is rebuilt from sp^3 to two-dimensional sp^2 hybrids. In the passivated

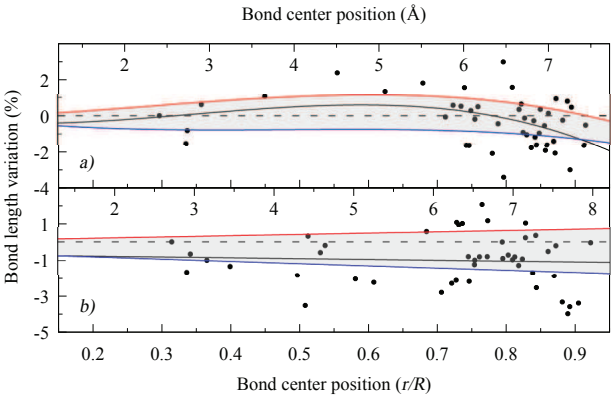

Fig. 2. (Color online) Dependence of the change in the length of the Cd–Te chemical bonds with respect to the central bond length (dots) on their relative position in the cluster (*a*) – unpassivated cluster, (*b*) – passivated one. Black solid lines – average deviations, red (dashed) lines – positive average deviations only, blue (dash-dotted) – negative average deviations only. Black dashed lines indicate the zero variation

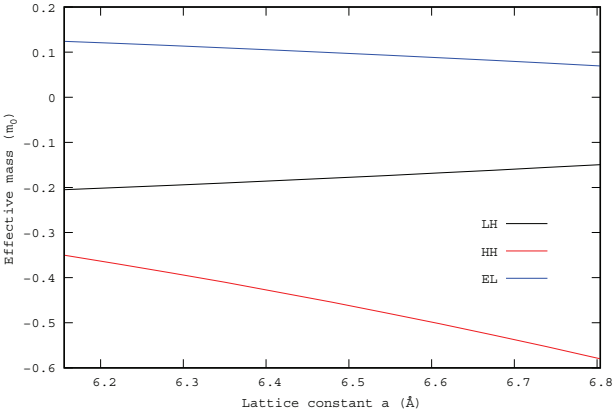

Fig. 3. (Color online) Dependence of the effective mass of the electron (EL), light (LH), and heavy (HH) holes on the lattice constant value of bulk cadmium telluride

cluster (Fig. 2, *b*), the bond length is distributed much more uniformly, although it also decreases by approaching the surface. The red line grows slightly in this case, while the blue one falls somewhat more strongly. As a result, the overall average (black line) is very close to the blue one. This distribution could be properly described by a linear approximation, while, in an unpassivated cluster, the polynomial of at least the 3$^{\text{rd}}$ order or even more complex function is needed for such a description. Although the maximum negative deviation is greater than that in the unpassivated cluster, the deviation does not exceed, in general, 5% of the central bond length. Some authors [26] showed that, for CdSe NPs, the value of a relaxation/reconstruction on the surface can reach 25% for the bond length and 25° for the angle value. In our opinion, such deviations are possible, if we are talking about the interatomic distance. However, the question arises: whether the chemical bond is preserved in this case? The answer to such a question is not clear, since the estimation of the "strength" of a chemical bond is not defined well from the point of view of quantum chemistry.

4. Spectra of Quasiparticles in Quantum Dots

For quantum dots, which are assumed to be homogenious and have a constant effective mass, the mathematical apparatus is well developed and, in most cases, allows one to obtain analytic solutions of the corresponding Schrödinger equation. In addition, the analytic solutions can be obtained for systems in which the effective mass accepts the fixed values in different regions, for instance, in multilayer quantum dots (core-shell systems). This, in turn, allows one to describe qualitatively a large number of effects occurring in quantum-dimensional systems. However, if the quasiparticle has a coordinate-dependent mass, the problem becomes much more complicated, although, in some cases, it can be solved [27, 28], and analytic solutions can be obtained.

In the absence of the spin-orbit interaction, electron and hole bands of cadmium telluride in a vicinity of Γ-point have a quadratic dependence on the quasivector $\mathbf{k}$. We calculated the effective mass via approximating the dispersion $E(\mathbf{k}) = \hbar^2\mathbf{k}^2/2m^*$ of the corresponding bands of electrons and heavy and light holes by a quadratic law at 21 $\mathbf{k}$ points in the interval of the wave vector modulus values (–0.005–0.005)$(2\pi/a)$, calculated for the set of values of the lattice constant a. Band structure calculations were performed within the LDA approximation in the plane wave basis, as described in Section 2. For calculations, we used a cubic unit cell containing 4 atoms of cadmium and 4 atoms of tellurium. For each value of the lattice constant, the geometric optimization of the atomic structure was carried out until the Hellmann–Feynman forces became less than 10^{-4} a.o. The result is presented in Fig. 3 for the interval of lattice constant values within ±5% of the experimental value

$a = 6.48$ Å. Hole masses are shown with a negative sign, what reflects the negative energies with respect to the valence band top. But, in the following, their absolute values are used. As can be seen from the figure, the effective masses of the electron m_e^* and the light hole m_{lh}^* are monotonically decreasing functions of the lattice constant, while the effective mass of the heavy hole m_{hh}^* – monotonically increasing. For the experimental value of the lattice constant, the values of the effective masses $m_e^* = 0.099\, m_0$ and $m_{hh}^* = 0.455\, m_0$ for the electron and the heavy hole, respectively, were obtained.

The Schrödinger equation for the motion of a particle with a mass that depends on its position in space, in a potential well, can be written in the form [29]:

$$\left\{-\frac{\hbar^2}{2}\left[\boldsymbol{\nabla}\frac{1}{m^*(\mathbf{r})}\boldsymbol{\nabla}\right] + V(\mathbf{r})\right\}\Psi(\mathbf{r}) = E\Psi(\mathbf{r}). \qquad (1)$$

Here, the effective mass $m^*(\mathbf{r})$ and the external potential $V(\mathbf{r})$ are functions of the spatial coordinates. In the case of spherical symmetry, they depend on the radial variable. Then, writing equation (1) in the spherical coordinate system, we can separate the radial and angular coordinates and find a solution in the form $\Psi(\mathbf{r}) = \psi(r)Y_{lm}(\Theta, \phi)$. Introducing the notations $\psi(r) = \phi(r)/r$, $m^{*\prime}(r) = dm^*(r)/dr$ and performing simple mathematical transformations (multiply by r^2 and divide by $m^*(r)$), the radial Schrödinger equation could be obtained in the following form:

$$\left\{\frac{d^2}{dr^2} - \frac{l(l+1)}{r^2} + \frac{m^{*\prime}(r)}{m^*(r)}\left(\frac{1}{r} - \frac{d}{dr}\right) - \right.$$
$$\left. - \frac{2m^*(r)}{\hbar^2}\left[V(r) - E\right]\right\}\phi(r) = 0. \qquad (2)$$

For the given cluster material, the dependence of the electron $m_e^*(r)$ and heavy hole $m_{hh}^*(r)$ effective masses on the radial variable in the spherical coordinate system can be obtained using the data presented in Figs. 2 and 3: by expressing the Cd-Te chemical bond length as a function of the radial coordinate $a_{\text{bond}}(r)$, it is possible to associate each value of the bond length with a specific lattice constant. In such a way, we obtain the dependence $a(r)$. In turn, each value of the lattice constant corresponds to a certain value of the effective mass $m^*(a)$. If to approximate accurately enough both dependencies with analytic functions (we used polynomials of the first, second, and third orders), then, by substituting one function into another one, we can get an analytic expression for the dependence $m^*(r)$. We determined the lattice constant using the fact that the optimized clusters have the zinc blende crystal structure: $a(r) = 4a_{\text{bond}}(r)/\sqrt{3}$. Such obtained dependencies of the effective masses of the electron and the heavy hole are shown in Figs. 4, *a* and 4, *d*, respectively. Black lines correspond to the unpassivated $Cd_{33}Te_{33}$ cluster, red lines to the $Cd_{33}Te_{33} : (SCH_3)_{21}$ cluster. As is seen, for a passivated cluster, the dependences of the electron and hole effective masses are close to linear ones, while, for an unpassivated one, these dependencies are much more complicated.

Equation (2) can be solved analytically only in certain cases, for example, for a specific analytic form of $m^*(r)$ [27, 28, 30]. In view of the complexity of the dependence of the effective mass and its derivative on the radial coordinate, it is rational to solve Eq. (2) numerically. In the simplest approximation of infinitely high potential barriers, the boundary conditions for the reduced wave function $\phi(r)$ are trivial: $\phi(0) = 0$, $\phi(R) = 0$, where R is the radius of the quantum dot. This makes it possible to use various numerical methods, in particular, the "shooting method", and, in such a way, to find the unknown energies E and reduced wave functions $\phi(r)$, and therefore $\psi(r)$, in a tabulated form.

Figure 4 shows the squares of the normalized radial wave functions $\psi(r)$ of an electron and a hole in the ground states ($n = 0$, $l = 0$) calculated for $Cd_{33}Te_{33}$ clusters, which are unpassivated or passivated by fragments of thiol-glycolic acid SCH_3. The black lines correspond to the normalized functions $\psi^{\text{const}}(r) = J_0(\sqrt{2m^*/\hbar^2 E}r)$, where $J_0(r)$ – spherical Bessel function, which is an analytic solution of Eq. (2) for the case of constant effective mass and infinitely high potential barriers:

$$\left\{\frac{d^2}{dr^2} - \frac{l(l+1)}{r^2} + \frac{2m^*}{\hbar^2}E\right\}R(r) = 0. \qquad (3)$$

The effective mass of an electron or hole is defined as the effective mass corresponding to the average length of chemical bonds (lattice constant). For an unpassivated cluster, the average length of a chemical bond is $a = 2.885$ Å, which gives the values of the effective masses $m_e^* = 0.083\, m_0$ and $m_{hh}^* = 0.523\, m_0$. For the passivated cluster, the values $a = 2.91$ Å,

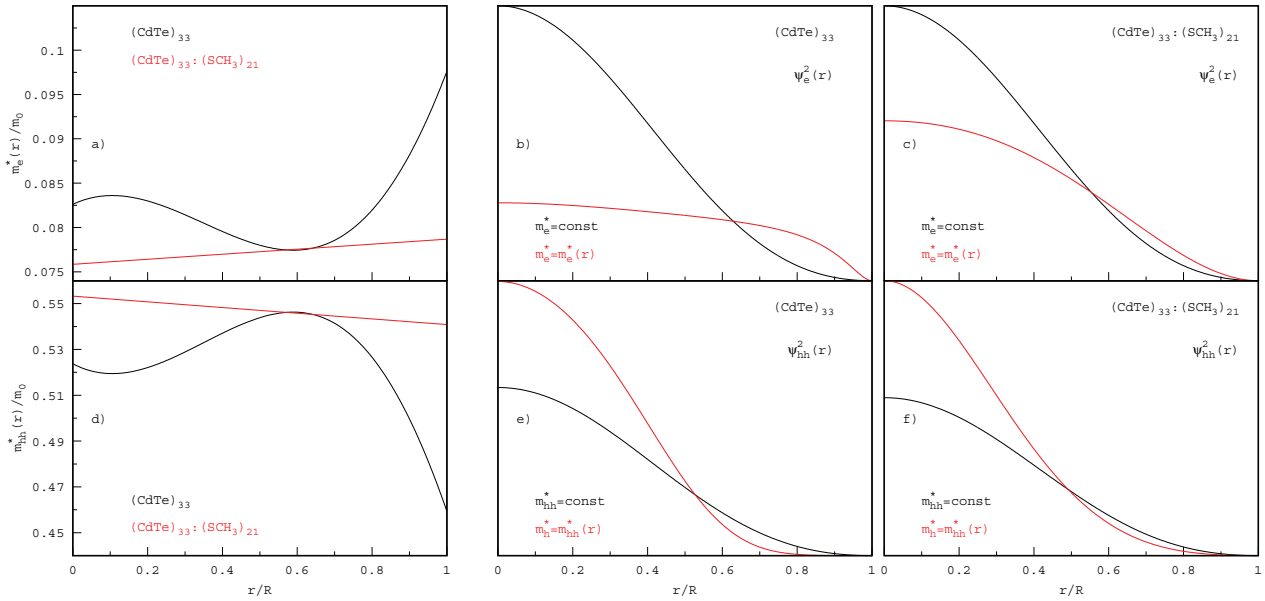

Fig. 4. (Color online) Dependence of the value of the effective mass of an electron (*a*) and a heavy hole (*d*) of the cluster area material on the relative position of this area in the cluster. (*b, c, e, f*) – the squared normalized radial wave function of the ground state of an electron and a heavy hole in the cluster (see text for details)

$m_e^* = 0.078\,m_0$ and $m_{hh}^* = 0.546\,m_0$, respectively, are obtained. Since both clusters have different radii, even under the condition of the same value of the effective mass (say, its bulk experimental value), different energy values are obtained as the solutions of Eq. (3): $E_{e,hh}^{\text{const}} = \hbar^2\pi^2/(2R^2 m_{e,hh}^*)$.

The calculated energies of the electron and hole in the ground states are shown in Table. Indeed, the energies of both the electron and the hole with a constant effective mass differ somewhat for different clusters, although this difference is small because of a small difference in the radii of the clusters ∼0.5 Å. The values of the average effective masses for both clusters are also quite similar. Therefore, as can be seen from Fig. 4, *b* and 4, *c*, the wave function of an electron with a constant mass has a very similar shape

Ground state energies of the electron and hole (eV)

Energy	$Cd_{33}Te_{33}$		$Cd_{33}Te_{33}:(SCH_3)_{21}$	
	$m^* = \text{const}$	$m^* = m^*(r)$	$m^* = \text{const}$	$m^* = m^*(r)$
E_e	6.870	1.814	6.488	2.134
E_{hh}	1.089	1.231	0.923	1.948

in both clusters. The effective mass of the electron is small in this case. Therefore, it has a high energy and is weakly localized in the region of the cluster (potential well). With regard for the dependence of the effective mass on the position in the cluster, the energy of the electron decreases by three times for passivated and four times for unpassivated clusters. However, the wave function, instead of becoming more localized, on the contrary, becomes more smooth in the region of the potential well. This is even more pronounced for the unpassivated cluster. Obviously, the effective mass of the electron decreases with a decrease in the radial coordinate (Fig. 3, *a*). Therefore, the energy of the electron increases, leading to a decrease in the localization of the wave function. For the hole states, the situation is the opposite: the effective mass of the hole increases when approaching the center of the cluster (Fig. 3, *d*), which leads to a decrease in the energy and, accordingly, an increase in the localization of the wave function. Indeed, as is seen from Figs. 4, *e* and 4, *f*, the wave function of a hole with a position-dependent effective mass (red line) for both clusters is more localized than the wave function of a hole with constant effective mass (black line). Herewith, the energy of the hole increases, but changes much weaker than for electrons: as is seen

from Table, for a passivated cluster, the energy differs twice, while, for an unpassivated one, the changes are much smaller.

5. Conclusions

The calculations within the density functional method demonstrate the dependence of the length of chemical bonds on their position in the cluster. For passivated clusters, the faces are formed on the surface, which is reflected in the calculated bond distribution. For passivated clusters, such faces are absent. Phenomenological models (the effective mass method) are applied with the assumption that the material of the cluster (quantum dot) retains its bulk characteristics. Taking the distribution of chemical bonds into account allows us to establish the corresponding distribution of the lattice constant and, therefore, of the effective mass in the cluster, and to perform calculations of the electronic and hole states with effective masses that depend on the position in the cluster. It is shown that the consideration of the dependence of the effective mass on the position in the cluster leads to a significant decrease in the energy of the electron (by several times) with respect to that with a fixed effective mass, as well as to a decrease in the localization of its wave function. For hole states with regard for the dependence of the effective mass on the position, we have shown that the energies increase slightly, and their wave functions become more localized.

The authors are sincerely grateful to the Armed Forces of Ukraine for the opportunity to conduct the scientific research in Kyiv.

1. D. Korbutiak, O. Kovalenko, S. Budzuliak, O. Melnychuk. *Nanostructures of A_2B_6 semiconductors: Monograph* (Nizhyn Mykola Gogol State University, 2020) [ISBN: 978-617-527-223-7].
2. Z. Pan, H. Rao, I. Mora-Seró, J. Bisquert, X. Zhong. Quantum dot-sensitized solar cells. *Chem. Soc. Rev.* **47**, 7659 (2018).
3. Y. Zhou, H. Zhao, D. Ma, F. Rosei. Harnessing the properties of colloidal quantum dots in luminescent solar concentrators. *Chem. Soc. Rev.* **47**, 5866 (2018).
4. H. Zhao, F. Rosei. Colloidal Quantum dots for solar technologies. *Chem.* **3**, 229 (2017).
5. D. Korbutyak, O. Kovalenko, S. Budzulyak, S. Kalytchuk, I. Kupchak. Light-emitting properties of A_2B_6 semiconductor quantum dots. *Ukr. J. Phys. Reviews* **7**, 48 (2012).
6. A. Dmytruk, I. Dmitruk, Y. Shynkarenko, R. Belosludov, A. Kasuya. ZnO nested shell magic clusters as tetrapod nuclei. *RSC Adv.* **7**, 21933 (2017).
7. N.V. Bondar, M.S. Brodyn, N.A. Matveevskaya, T.G. Beynik. Efficient and sub-nanosecond resonance energy transfer in close-packed films of ZnSe quantum dots by steady-state and time-resolved spectroscopy. *Superlattices and Microstructures* **138**, 106382 (2020).
8. A.E. Raevskaya, O.L. Stroyuk, D.I. Solonenko, V.M. Dzhagan, D. Lehmann, S.Y. Kuchmiy, V.F. Plyusnin, D.R.T. Zahn. Synthesis and luminescent properties of ultrasmall colloidal CdS nanoparticles stabilized by Cd(II) complexes with ammonia and mercaptoacetate. *J. Nanopart. Res.* **16**, 2650 (2014).
9. N. Reilly, M. Wehrung, R.A. O'Dell, L. Sun. Ultrasmall colloidal PbS quantum dots. *Mater. Chem. Phys.* **147**, 1 (2014).
10. F. Cheng, M. Yu, L. Jia, Q. Tian, J. Zhang, B. Kim, X. Zhao. Ultra-small PbSe quantum dots synthesis by chemical nucleation controlling. *J. Wuhan University of Technology–Mater. Sci. Ed.* **36**, 478 (2021).
11. B. Talluri, E. Prasad, T. Thomas. Ultra-small ($r < 2$ nm), stable (>1 year) copper oxide quantum dots with wide band gap. *Superlattices and Microstructures* **113**, 600 (2018).
12. M. Valakh, V. Dzhagan, A. Raevskaya, S. Kuchmiy. Optical investigations of ultra-small colloidal nanoparticles and heteronanoparticles based on II–VI semiconductors. *Ukr. J. Phys.* **56**, 1080 (2022).
13. A.L. Rogach, A. Kornowski, M. Gao, A. Eychmüller, H. Weller. Synthesis and characterization of a size series of extremely small thiol-stabilized CdSe nanocrystals. *J. Phys. Chem. B* **103**, 3065 (1999).
14. T. Takagahara. Effects of dielectric confinement and electron-hole exchange interaction on excitonic states in semiconductor quantum dots. *Phys. Rev. B* **47**, 4569 (1993).
15. I.M. Kupchak, Y.V. Kryuchenko, D.V. Korbutyak, A.V. Sachenko, E.B. Kaganovich, E.G. Manoilov, E.V. Begun. Exciton states and photoluminescence of silicon and germanium nanocrystals in an Al_2O_3 matrix. *Semiconductors* **42**, 1194 (2008).
16. R. Arraoui, A. Sali, A. Ed-Dahmouny, M. Jaouane, A. Fakkahi. Polaronic mass and non-parabolicity effects on the photoionization cross section of an impurity in a double quantum dot. *Superlattices and Microstructures* **159**, 107049 (2021).
17. F. Long, W.E. Hagston, P. Harrison, T. Stirner. The structural dependence of the effective mass and Luttinger parameters in semiconductor quantum wells. *J. Appl. Phys.* **82**, 3414 (1997).
18. S.K. Bhattacharya, A. Kshirsagar. Ab initio calculations of structural and electronic properties of CdTe clusters. *Phys. Rev. B* **75**, 035402 (2007).
19. M.M. Sigalas, E.N. Koukaras, A.D. Zdetsis. Size dependence of the structural, electronic, and optical properties

of (CdSe) n, n = 6–60, nanocrystals. *RSC Advances* **4**, 14613 (2014).
20. P.J. Stephens, F.J. Devlin, C.F. Chabalowski, M.J. Frisch. Ab initio calculation of vibrational absorption and circular dichroism spectra using density functional force fields. *J. Phys. Chem.* **98**, 11623 (1994).
21. W.R. Wadt, P.J. Hay. Ab initio effective core potentials for molecular calculations. Potentials for main group elements Na to Bi. *J. Chem. Phys.* **82**, 284 (1985).
22. M.W. Schmidt, K.K. Baldridge, J.A. Boatz, S.T. Elbert, M.S. Gordon, J.H. Jensen, S. Koseki, N. Matsunaga, K.A. Nguyen, S. Su *et al.* General atomic and molecular electronic structure system. *J. Computational Chem.* **14**, 1347 (1993).
23. P. Giannozzi, O. Baseggio, P. Bonfà, D. Brunato, R. Car, I. Carnimeo, C. Cavazzoni, S. de Gironcoli, P. Delugas, F. Ferrari Ruffino *et al.* Quantum ESPRESSO toward the exascale. *J. Chem. Phys.* **152**, 154105 (2020).
24. J.D. Pack, H.J. Monkhorst. "Special points for Brillouin-zone integrations" – a reply. *Phys. Rev. B* **16**, 1748 (1977).
25. M. Methfessel, A.T. Paxton. High-precision sampling for Brillouin-zone integration in metals. *Phys. Rev. B* **40**, 3616 (1989).
26. A. Puzder, A. J. Williamson, F. Gygi, G. Galli. Self-healing of CdSe nanocrystals: first-principles calculations. *Phys. Revi. Lett.* **92**, 1 (2004).
27. A. Keshavarz, N. Zamani. Optical properties of spherical quantum dot with position-dependent effective mass. *Superlattices and Microstructures* **58**, 191 (2013).
28. H. Sari, E. Kasapoglu, S. Sakiroglu, I. Sökmen, C.A. Duque. Effect of position-dependent effective mass on donor impurity-and exciton-related electronic and optical properties of 2D Gaussian quantum dots. *Europ. Phys. J. Plus* **137**, 341 (2022).
29. J.-M. Lévy-Leblond. Position-dependent effective mass and Galilean invariance. *Phys. Rev. A* **52**, 1845 (1995).
30. M. Sebawe Abdalla, H. Eleuch. Exact solutions of the position-dependent-effective mass Schrödinger equation. *AIP Advances* **6**, 055011 (2016).

Received 07.11.22

І.М. Купчак, Д.В. Корбутяк

СПЕКТРАЛЬНІ ХАРАКТЕРИСТИКИ ПАСИВОВАНИХ КВАНТОВИХ ТОЧОК CdTe З КООРДИНАТНО-ЗАЛЕЖНИМИ ПАРАМЕТРАМИ

Теоретичні дослідження енергетичного спектра квантових точок часто проводяться методом ефективної маси, у якому відповідні параметри розрахунку задаються об'ємними значеннями матеріалу як самої точки, так і її оточення. В даній роботі ефективна маса є координатно-залежною функцією, а її залежність від координати визначено виходячи з атомної структури квантової точки, яка, у свою чергу, розрахована методом функціонала густини. Розглянуто як непасивовані, так і квантові точки, пасивовані тіол-гліколевою кислотою.

Ключові слова: квантові точки, координатно-залежна ефективна маса, телурид кадмію.